RIPK3 modulates sarcoma through immune checkpoint *HAVCR2*

CHEN QIAN, DELUO WU and JIANWEI DU

Department of Orthopedics, Affiliated Hospital of Yangzhou University, Yangzhou, Jiangsu 225000, P.R. China

Received March 23, 2022; Accepted August 11, 2022

DOI: 10.3892/ol.2022.13501

Abstract. Sarcomas is a complex group of malignant diseasse with undetermined molecular mechanisms. Receptor interacting serine/threonine kinase 3 (*RIPK3*) is a necroptosis- and apoptosis-related marker that has been implicated in several immune-associated diseases and aggressive malignant tumours. In the present study, publicly available transcriptome sequencing data were collected from The Cancer Genome Atlas (TCGA) and Therapeutically Applicable Research To Generate Effective Treatments (TARGET) databases and extensive data mining was performed, focusing on *RIPK3* and its potential function in the modulation of gene expression and signaling pathways, immune checkpoints and cell infiltration. Analysis of TCGA and TARGET data revealed 603 up- and 260 downregulated genes in the higher *RIPK3* expression group compared with the lower *RIPK3* expression groups, with transmembrane channel like 8 and transmembrane protein 97 as the top up- and downregulated genes, respectively. Further pathway analysis revealed that the overexpressed genes were enriched in 'cytokine-cytokine receptor interaction'. Higher *RIPK3* was found to be associated with improved survival, the immune checkpoint gene hepatitis A virus cellular receptor 2 (*HAVCR2*) and an improved response to immune blockade therapy. The potential modulation of *HAVCR2* expression by *RIPK3* was confirmed by reverse transcription-quantiative PCR in KHOS and 143B human osteosarcoma cell lines. Immune cell infiltration analysis revealed that *RIPK3* was positively associated with macrophage and monocyte infiltration, suggesting that *RIPK3* executes its function through these immune cells. These findings led to the hypothesis that increased *RIPK3* expression may result in improved survival, possibly by regulating the immune checkpoint *HAVCR2*. In conclusion, the present study comprehensively elucidated the *RIPK3* profile with regard to sarcoma survival, transcriptome expression, immune checkpoint therapy and immune cell infiltration. These findings suggest that *RIPK3* is potentially a therapeutic target for sarcoma.

Correspondence to: Professor Jianwei Du, Department of Orthopedics, Affiliated Hospital of Yangzhou University, 45 Taizhou Road, Yangzhou, Jiangsu 225000, P.R. China
E-mail: doctorduyz@163.com

Key words: RIPK3, sarcoma, *HAVCR2*

Introduction

Sarcoma is a complex group of malignant diseases consisting of >100 disease subtypes, most of which vary according to the tissue and cell context, which include bone, cartilage, kidney, adipose, colon, connective, subcutaneous and other soft tissues. The prevalence of sarcoma varies across different subgroups, but its overall prevalence among all malignancies worldwide is <1% in adults and 6% in teenagers. Among all subtypes, soft tissue sarcomas (STSs) are likely to have a higher incidence than other subtypes. STSs can affect any part of the human body, with the most frequent locations being the upper and lower limbs (1). The distant metastases of STS generally occur in the lung, bone and liver, while regional lymph node metastasis is less common (2).

The etiology of sarcoma is largely unknown, but evidence suggests that genetic and epigenetic components contribute significantly to disease phenotypes (3-5). During the past 10 years, several genetic evaluations have revealed that nucleotide variations, germline or somatic mutations, certain indels or deletions, copy number variations and chromosomal translocations (CNVs) are associated with sarcoma (6). For example, mutations in the tumor protein 53, ATRX chromatin remodeler and RB transcriptional corepressor 1 genes are commonly detected in all subtypes. These three genes play roles in the regulation of the cell cycle and chromosomal stability. Some CNVs in cyclin dependent kinase inhibitor 2, *CDK4* and MDM2 proto-oncogene also contribute to the disease manifestations, according to a recent genetic architecture report of sarcoma published by The Cancer Genome Atlas (TCGA) (7).

Receptor interacting serine/threonine kinase 3 (*RIPK3*) encodes a receptor-interacting protein that acts a regulator of necroptosis and apoptosis (8). *RIPK3* has been implicated to serve a critical role in several inflammatory disorders, including bowel diseases, psoriasis, systemic inflammatory response syndrome and severe cancers (9-11). Its capacity to activate necroptosis through the inflammasome has been confirmed by several research groups. However, its function in sarcoma remains largely unknown. In the current study, by retrieving the TCGA dataset, a comprehensive evaluation of the association of *RIPK3* expression level with survival, transcriptome alteration, signalling pathways, immune checkpoint therapy and immune cell infiltration of sarcoma was performed. In addition, the regulatory effect of *RIPK3* on the immune checkpoint gene hepatitis A virus cellular receptor 2 (*HAVCR2*) was investigated.

Materials and methods

Data retrieval. Data were retrieved from the Gene Expression Omnibus dataset GSE49972 and TCGA dataset (accession no. phs000178.v11.p8). GSE49972 includes data for 22 clear cell sarcoma of the kidney tissues and 10 non-neoplastic kidney tissues, while phs000178 includes 260 samples of a wide range of sarcoma subtypes and a large amount of comprehensive clinical data. In addition, RNA-seq data were extracted from the Therapeutically Applicable Research To Generate Effective Treatments (TARGET) program (https://target-data.nci.nih.gov/Public/OS/mRNA-seq/). In GSE49972 the expression levels were evaluated using the HumanHT-12 v4 Expression BeadChip (12). Transcriptome data in dataset phs000178 were generated using a HiSeq 2000 sequencing system with 76 bp paired-end parallel sequencing. The RNA-seq data of 89 sarcoma samples in TARGET were assayed by parallel sequencing with an Illumina Genome Analyzer IIx, Illumina HiSeq 2000 or Illumina MiSeq sequencer.

Survival and prognosis. Transcriptome read levels of *RIPK3*, survival, sex and age were extracted from TCGA (https://portal.gdc.cancer.gov/) or the National Center for Biotechnology (NCBI) databank (https://www.ncbi.nlm.nih.gov). Individuals were divided into high and low expression groups ($RIPK3^{higher}$ and $RIPK3^{lower}$) according to the expression level of *RIPK3*. The Kaplan-Meier algorithm was used to construct survival curves for the *RIPK3* high and low groups, and the nonparametric log-rank test was used to calculate the statistical significance of differences in survival. HR represents chance of death occurring in the $RIPK3^{higher}$ group compared with the $RIPK3^{lower}$group. HR >1 indicates that *RIPK3* is a risk factor, while HR <1 indicates that *RIPK3* has a protective role. The median survival time was set at the time of 50% survival for each group. Time-dependent receiver operating characteristic (ROC) analysis was carried out to predict the accuracy of the RIPK3 prediction. In this analysis, the larger the area under the curve (AUC) the more robust the prediction model.

Univariate and multivariate Cox proportional hazards regression models were used to determine the independent prognostic factors using the survminer_0.4.9 R package (https://github.com/kassambara/survminer). The forestplot_2.0.1 package (https://cran.r-project.org/web/packages/forestplot/index.html) was used to generate the P-value, HR and 95% CI of each variable. A nomogram was created based on the results of the multivariate Cox proportional hazards analysis to predict the 1-, 3- and 5-year overall recurrence, which was indicated by the points associated with each risk factor through the rms_6.3-0 R package (https://cran.r-project.org/web/packages/rms/index.html).

Identification of differentially expressed genes. Genome-wide mRNA expression data were obtained from the phs000178 and TARGET datasets. The expression levels between the $RIPK3^{higher}$ and $RIPK3^{lower}$ groups were compared using the limma_3.40.2 R package (http://www.bioconductor.org/packages/release/bioc/html/limma.html). Significant differentially expressed genes were defined as having a fold change (FC) of >2 or <-2 and false discovery rate (FDR) adjusted P<0.05. A volcano plot was constructed with $\log_2$(FC) on the x-axis against -$\log_{10}$(FDR-adjusted P-value), in which each dot represents a single individual. A heatmap was generated with the top 50 up- and top 50 downregulated genes. For the differentially expressed genes, Kyoto Encyclopedia of Genes and Genomes (KEGG) and Gene Ontology (GO) analyses were performed using the clusterProfiler_3.18.0 R package (https://bioconductor.org/packages/release/bioc/html/clusterProfiler.html). GO annotation was divided into three separate parts: Molecular function, biological pathways and cellular components.

Cell culture and reverse transcription (RT)-PCR. The KHOS and 143B human osteosarcoma cell lines were gifts from the American Type Culture Collection cell bank. The cell lines were authenticated by STR genotyping and comparison with the relevant reference data in Cellosaurus (https://web.expasy.org/cellosaurus/). Cells were cultured in a humidified incubator at 37˚C with 5% CO_2 in DMEM (Gibco; Thermo Fisher Scientific, Inc) supplied with 10% FBS (Gibco; Thermo Fisher Scientific, Inc.), 0.015 mg/ml 5-bromo-2'-deoxyuridine, 100 U/ml penicillin and 100 μg/ml streptomycin. Cells were harvested when they reached 70-80 confluence in 15-cm dishes. GSK872 at concentrations of 100 nM and 1, 2, 4, 8 and 10 μM was added to the cultured cells and incubated for 2 h at 37˚C. The *HAVCR2* and *GAPDH* expression of GSK872-treated cells were compared with untreated cells as a control. The cells were then harvested and the expression levels of *HAVCR2* and *GAPDH* were assayed.

Total RNA was extracted from the cells with the RNeasy Protect Mini Kit (Qiagen) according to the manufacturer's protocols. Agarose gel electrophoresis was used to check the integrity of the RNA. The RNA was then reverse transcribed with the Third-Generation Reverse Transcription Master Mix according to the manufacturer's instructions (MR05001S; Monad Biotech Co., Ltd.). Quantitative expression primers for *HAVCR2* were designed using online tools from the Harvard website (https://pga.mgh.harvard.edu/primerbank/index.html). The forward and reverse primer sequences were as follows. *HAVCR2 forward* CTGCTGCTACTACTTACA AGGTC and reverse, GCAGGGCAGATAGGCATTCT. The forward primer was located at positions 40-62 and the reverse primer at positions 95-114 of the original *HAVCR2* mRNA sequence (accession no. NM_032782.5). The primers for the reference gene were: *GAPDH* forward, GGAGCG AGATCCCTCCAAAAT and reverse, GGCTGTTGTCAT ACTTCTCATGG. The final content of the qPCR product was 1X master mix, 0.2 μM forward and reverse primers, 1X low ROX dye, 50 ng cDNA and nuclease-free water to a total volume of 20 μl. The PCR steps were set as follows: Initial denaturation, 95˚C for 10 min; denaturation, 95˚C for 10 sec; and annealing and extension, 60˚C for 30 sec. There were 40 cycles of denaturation, annealing and extension. RT-PCR analysis was performed using an Applied Biosystems 7900HT Fast Real-Time PCR System.

RIPK3 and immunity. Immune checkpoint genes were selected from high-impact publication (13-15). The xCell algorithm combined bulk RNA-seq data as the sum of the expression in several single cell types in these samples (https://xcell.ucsf.edu). Then, reference gene expression profiles were established

for each major tumor-infiltrating immune cell type, i.e., CD4 T^+, CD8 T^+, B, natural killer (NK), neutrophils and macrophages (16). Spearman's correlation analysis was used to determine the correlation between quantitative variables and *RIPK3* expression. Tumor Immune Dysfunction and Exclusion (TIDE) scores were used to evaluate immune checkpoint blockade (ICB) therapy response. The TIDE scores were based on 189 human cancer studies and 33,197 samples (http://tide.dfci.harvard.edu/download/).

Statistical analysis. All statistical analyses were performed with R project version 4.0.3 (https://www.r-project.org). The ggrisk_1.3 (https://cran.r-project.org/web/packages/ggrisk/index.html), survival_3.3-1 (https://cran.r-project.org/web/packages/survival/index.html), survminer, timeROC_0.4 (https://cran.r-project.org/web/packages/timeROC/index.html) and rms packages were used for survival and prognosis analysis. Differences among multiple groups were analyzed using one-way ANOVA followed by Dunnett's post hoc test. Differences between two groups were analyzed using Wilcoxon's rank-sum test or two-sample (unpaired) t-tests.

Results

Higher RIPK3 is associated with improved survival in sarcoma. Expression data were retrieved from GSE49972, including data for 22 kidney sarcomas, 6 adult normal nonneoplastic kidneys and 4 fetal samples. The expression of *RIPK3* was significantly lower in the sarcoma patient group than in the normal group ($P=7x10^{-6}$; Fig. 1A). Due to the relatively limited sample size in this dataset, other datasets with larger sample sizes were also searched for. Under TCGA accession number phs000178, a transcriptome dataset of 260 patients with sarcoma was found. As the expression data of only two normal tissues were available in this dataset, it was not possible to compare the differences between case and normal groups. The transcripts per million expression datasets were retrieved and plotted against survival time and survival status for all patients (Fig. 1C). The samples were then classified into two groups: *RIPK3*^{higher} (above the median expression level) and *RIPK3*^{lower} (below the median expression level). The Kaplan-Meier survival curve indicated that patients in the *RIPK3*^{higher} survived for a longer time than those in the *RIPK3*^{lowe} group, with median survival times of 6.7 and 4.2 years, respectively [log-rank P=0.0012, HR(low exp)=1.958, 95% CI (1.302, 2.943); Fig. 1B)]. The AUC values were 0.64, 0.64 and 0.65 for 1 year, 3 years and 5 years, respectively (Fig. 1D). A similar trend was also identified using data from the TARGET database, which showed that patients in the *RIPK3*^{higher} group were likely to survive for a longer time than those in the *RIPK3*^{lower} group (median 9.2 vs. 7.2 years, respectively; Fig. S1), although the difference in survival between the groups was not found to be statistically significant. Since other *RIPK*s could potentially be involved in the necroptosis and apoptosis system, whether *RIPK1, RIPK2* and *RIPK4* were associated with the overall survival probability was also examined. However, there was no evidence to suggest that these other *RIPKs* were associated with improved or worse survival (Fig. S2). These data indicate that *RIPK3* may be associated with longer survival in sarcoma.

To further confirm the aforementioned findings, prognostic analysis was performed for the *RIPK3* gene, using age, sex and new tumor type as covariates. The results suggested that *RIPK3* may independently protect patients, following analysis using univariate and multivariate Cox regression models ($P_{uni-cox}=1.3x10^{-4}$, HR=0.66; $P_{multi-cox}=0.024$, HR=0.73; Fig. 2A and B). Based on the findings of the multivariate Cox proportional hazards analysis, a nomogram was built to predict the 1-, 3- and 5-year overall recurrence of each individual based on the assignment of points associated with each risk factor and the concordance index (C-index) was used to evaluate the predictive model. The C-index of 0.63 indicated a good predictive outcome (P<0.001; Fig. 2C and D). These data suggest that higher *RIPK3* may be a protective factor that is associated with an improved prognosis.

Expression profile of the RIPK3^{higher} *and RIPK3*^{lower} *groups*. Exploration of the expression landscape of the *RIPK3*^{higher} and *RIPK3*^{lower} groups will improve understanding of the functional role of *RIPK3* in sarcoma development. Therefore, the differential expression profiles were compared between the *RIPK3*^{higher} and *RIPK3*^{lower} groups from the phs000178 dataset. Applying stringent statistical criteria of a FC of >2 or <-2 and FDR adjusted P<0.05, a total of 863 differentially expressed genes were identified, including 603 up- and 260 downregulated genes (Fig. 3A, Table SI). Notably, the number of genes with upregulated expression was 2.3-fold that of genes with downregulated expression. For the 50 fifty up- and downregulated differentially expressed genes, 74.1% (192/259) of the sarcoma samples were successfully classified into *RIPK3*^{higher} and *RIPK3*^{lower} groups (Fig. 3B). The top up- and downregulated genes were transmembrane channel like 8 (*TMC8*; FDR-adjusted $P=2.62x10^{-31}$, log(FC)=1.7) and transmembrane protein 97 (*TMEM97*; FDR-adjusted $P=3.91x10^{-18}$, log(FC)=-1.1), respectively. To confirm these findings, the expression of these genes in the TARGET dataset was determined, and the results revealed that the expression of *TMC8* was significantly increased while the expression of *TMEM97* was decreased in the *RIPK3*^{higher} group compared with the *RIPK3*^{lower} group (Fig. S3). *TMC8* and *TMEM97* have both been implicated in cancer pathogenesis (17,18); however, they have not previously been identified as having an association with sarcoma. Therefore, these are suggested new targets that deserve further investigation in the future.

KEGG and GO functional annotation of the 603 up- and 260 downregulated genes revealed several signaling pathways that may be involved in *RIPK3*-associated disease pathogenesis. For the upregulated genes, 68 signaling pathways showed strong enrichment against background with the pathway hsa04640 'hematopoietic cell lineage' having the lowest P-value (GeneRatio=0.11, FDR-corrected $P=3.49x10^{-24}$). This pathway contains several cell surface markers (*CD2*, *CD4, CD5, CD7, CD14, CD33, CD37, CD55 and CD1C*) and major histocompatibility-related haplotypes [human leukocyte antigen (*HLA*)-*DPB1, HLA-DRB1, HLA-DRA/HLA-DPA1, HLA-DOA, HLA-DQA1, HLA-DRB5, HLA-DQB1, HLA-DOB* and *HLA-DQA2*]. Other top pathways included hsa04060 'cytokine-cytokine receptor interaction' and hsa04514 'cell adhesion molecules' (Table SII). The 260 downregulated genes were enriched in 25 pathways, with the top one being hsa04270

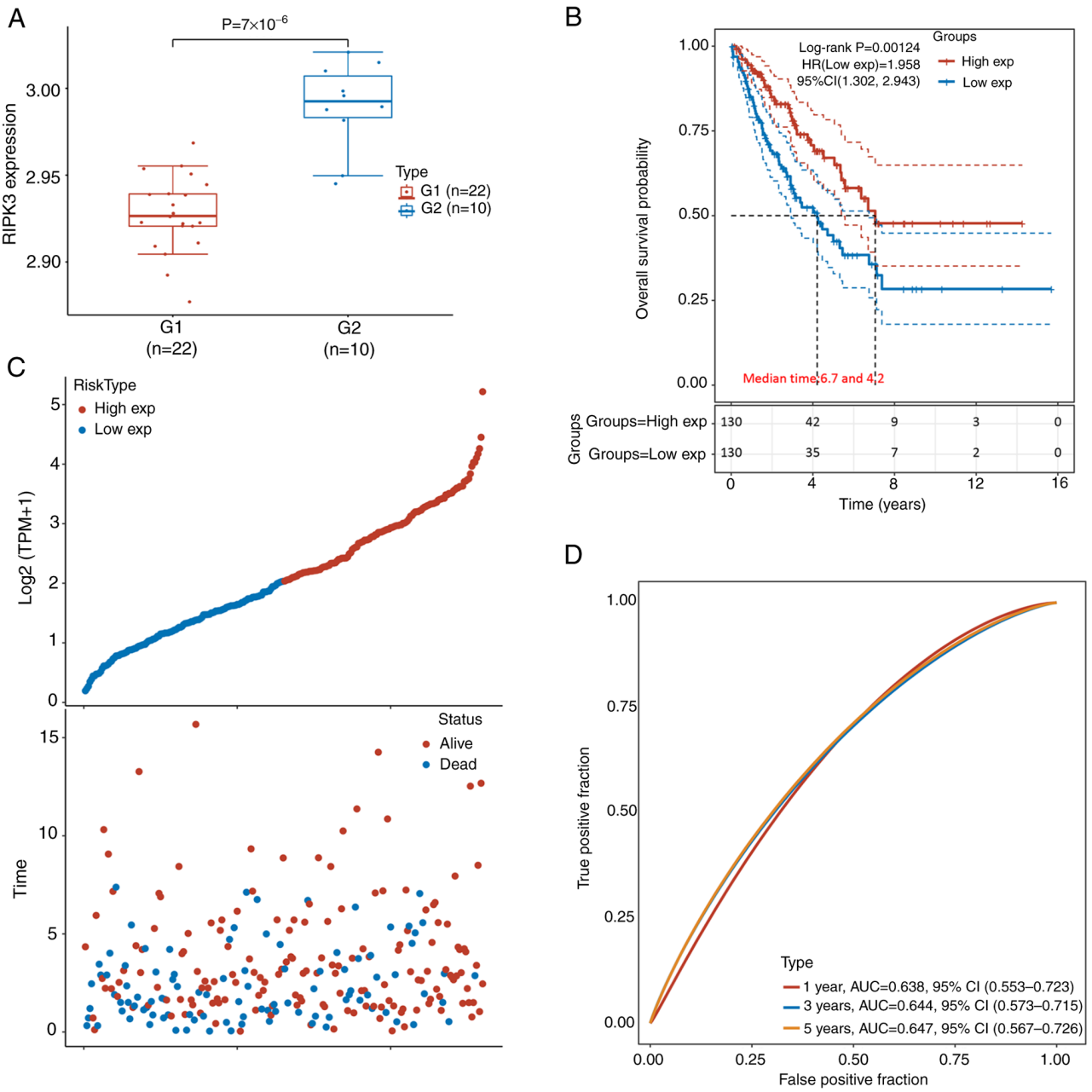

Figure 1. *RIPK3* is associated with sarcoma survival in The Cancer Genome Atlas dataset. (A) *RIPK3* was significantly downregulated in the patients with sarcoma compared with the control group (two-sample t-test). (B) Kaplan-Meier analysis revealed that the group with high *RIPK3* expression had increased survival compared with the group with low *RIPK3* expression. (C) *RIPK3* log2(TPM+1) expression data were separated into high (red dot) and low (blue dot) groups (upper panel), and into live (red dot) or dead (blue dot) groups (lower panel). The x-axis represents the rank for each sample from the lowest to highest expression of RIPK3. (D) Receiver operative curve analysis for 1, 3 and 5 years. *RIPK3*, receptor interacting serine/threonine kinase 3; G1, patients with sarcoma; G2, control group; exp, expression; TPM, transcripts per million; AUC, area under the curve.

'vascular smooth muscle contraction' (GeneRatio=0.13, FDR-corrected P=2.97x10^{-5}; Fig. 3C). To further validate these findings, the expression profiles of the *RIPK3*^{higher} and *RIPK3*^{lower} groups in the TARGET dataset were checked. A similar expression pattern was observed, which verified several of the enriched pathways or GO terms, particularly for the top pathway hsa04060 'cytokine-cytokine receptor interaction' and the GO terms 'response to interferon-gamma' and 'T cell activation' (Table SIII; Fig. S4). These data indicate that *RIPK3* may modulate gene expression and immune signaling pathways in sarcoma, reflecting some key features of sarcoma etiology.

RIPK3 is positively associated with HAVCR2. Since RIPK3 is indicated to be involved in cytokine-cytokine receptor interactions and to have a potential role in regulation of the immune response, the correlations between *RIPK3* and several immune checkpoint genes were evaluated. First, the expression levels of seven immune checkpoint genes [sialic acid binding Ig like lectin 15 (*SIGLEC15*), *CD274*, *HAVCR2*, T cell immunoreceptor with Ig and ITIM domains (*TIGIT*), cytotoxic T-lymphocyte associated protein 4 (*CTLA4*), lymphocyte-activation 3 and programmed cell death 1 ligand 2) were extracted. Spearman's correlation analysis showed that *RIPK3* was most strongly correlated with *HAVCR2*, *TIGIT* and *CTLA4* in the

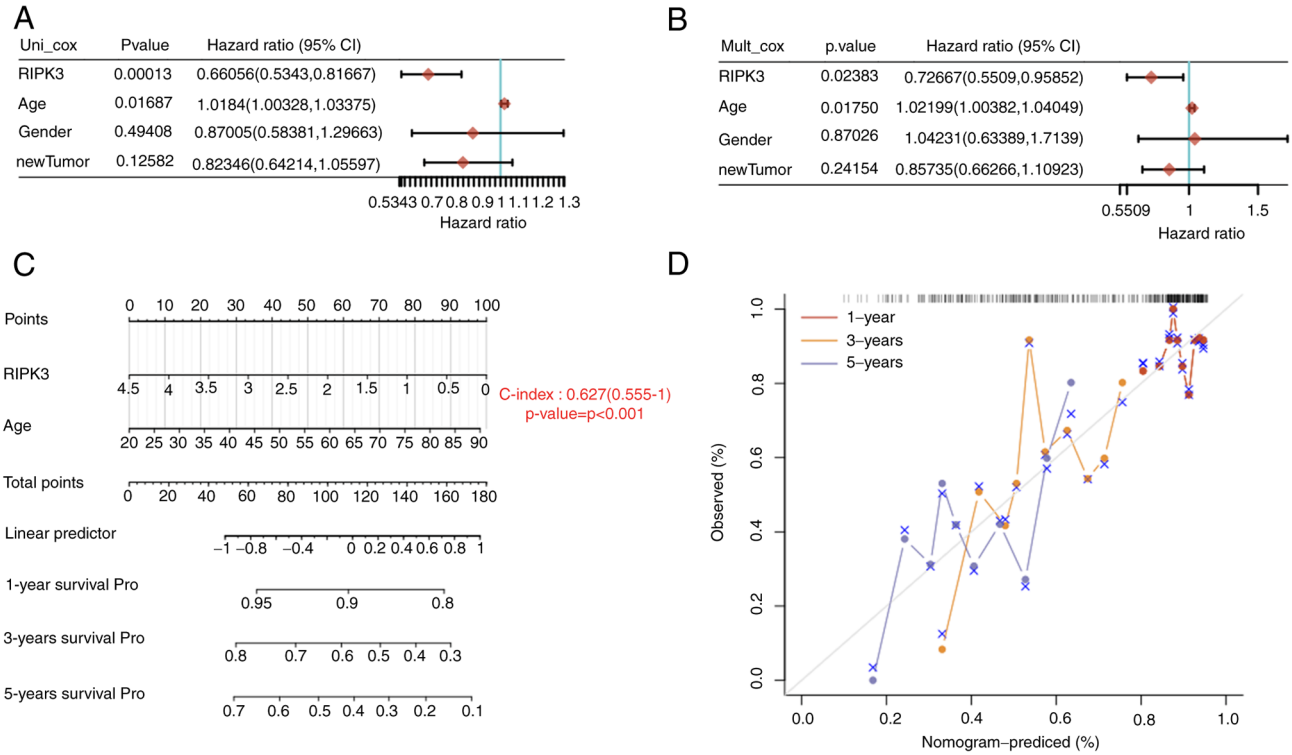

Figure 2. *RIPK3* contributes to an improved prognosis. *RIPK3* was shown to be associated with an improved prognosis using (A) univariate and (B) multivariate Cox regression analyses. (C) The C-index was used to evaluate the nomogram prediction model based on the expression of *RIPK3*. (D) Nomogram plot predicting the 1-, 3- and 5-year overall recurrence of each individual. RIPK3, receptor interacting serine/threonine kinase 3; uni, univariate; mult, multivariate; pro, probability.

TCGA dataset (correlation coefficient=0.63, 0.59 and 0.47, P=2.00x10^{-14}, 6.71x10^{-16} and 3.21x10^{-6}, respectively, Fig. 4A and B). Evaluation of the correlation between the above three genes and *RIPK3* in the TARGET dataset validated the positive correlation of *HAVCR2* with *RIPK3* (correlation coefficient=0.41, P=3.50x10^{-5}; Fig. 4C and D).

To determine whether *RIPK3* induces the expression of *HAVCR2*, two osteosarcoma cell lines, KHOS and 143B, were treated with the *RIPK3* inhibitor GSK872 and *HAVCR2* expression was detected using RT-qPCR. Information was sought regarding the GSK872 concentration that would sufficiently inhibit *RIPK3* activity. A literature search on NCBI indicated that 1-10 μM GSK872 fully inhibited RIPK3 activity (19-21). The *HAVCR2* expression level was empirically tested following treatment of the two cell lines with 100 nM -10 μM GSK872. The results indicate that *HAVCR2* expression was decreased in the KHOS and 143B lines when the cells were treated with ≥2 μM GSK872, suggesting that *RIPK3* might positively regulate *HAVCR2* expression (Fig. 4E).

To confirm the important roles of *RIPK3* in sarcoma, the TIDE algorithm was used to predict potential ICBs. The TIDE algorithm is a statistical method for the modelling of immune evasion from two relevant perspectives: i) the induction of T-cell dysfunction with high infiltration of cytotoxic T lymphocytes (CTLs) and ii) the prevention of T-cell infiltration with low CTL levels. The higher the TIDE score, the worse the response to ICB therapy (22). The TIDE scores in the RIPK3^{higher} group were slightly higher than those in the *RIPK3*^{lower} group, indicating that *RIPK3*^{high} patients would benefit more from ICB therapy (P=0.05; Fig. 4F). In summary, these data suggest that *RIPK3* may regulate *HAVCR2* and could serve as an ICB response marker.

RIPK3 is associated with macrophage and monocyte infiltration. Next, whether immune cell subtypes contribute to sarcoma development was investigated. Using an xCell algorithm to calculate immune cell infiltration, the abundance of immune cell types was successfully derived using a reference set with 46 immune cell subtypes for the *RIPK3*^{higher} and *RIPK3*^{lower} groups (including endothelial cells, macrophages, B cells, NK cells, CD4$^+$ T cells and CD8$^+$ T cells; Table SIV). xCell is based on a spillover compensation technique in which reference gene signatures of each immune cell type are built from RNA-Seq samples of various human innate and adaptive circulating immune cells (23). Using this strategy, significant differences in macrophage and monocyte infiltration were observed between the *RIPK3*^{higher} and *RIPK3*^{lower} groups in the TCGA database (P<2.2x10^{-16} for both monocytes and macrophages; Fig. 5A). These findings were verified in the TARGET database, with significantly higher macrophage and monocyte infiltration in the RIPK3^{higher} group (Fig. 5B, Table SV). In summary, these data suggest that *RIPK3* may modulate disease through effects on macrophages and monocytes, suggesting a potential target for the regulation of sarcoma development.

Discussion

In the current study, evidence that *RIPK3* might modulate sarcoma development through the immune checkpoint *HAVCR2* was presented. Notably, *RIPK3* expression was associated with immune scores in macrophages and monocytes,

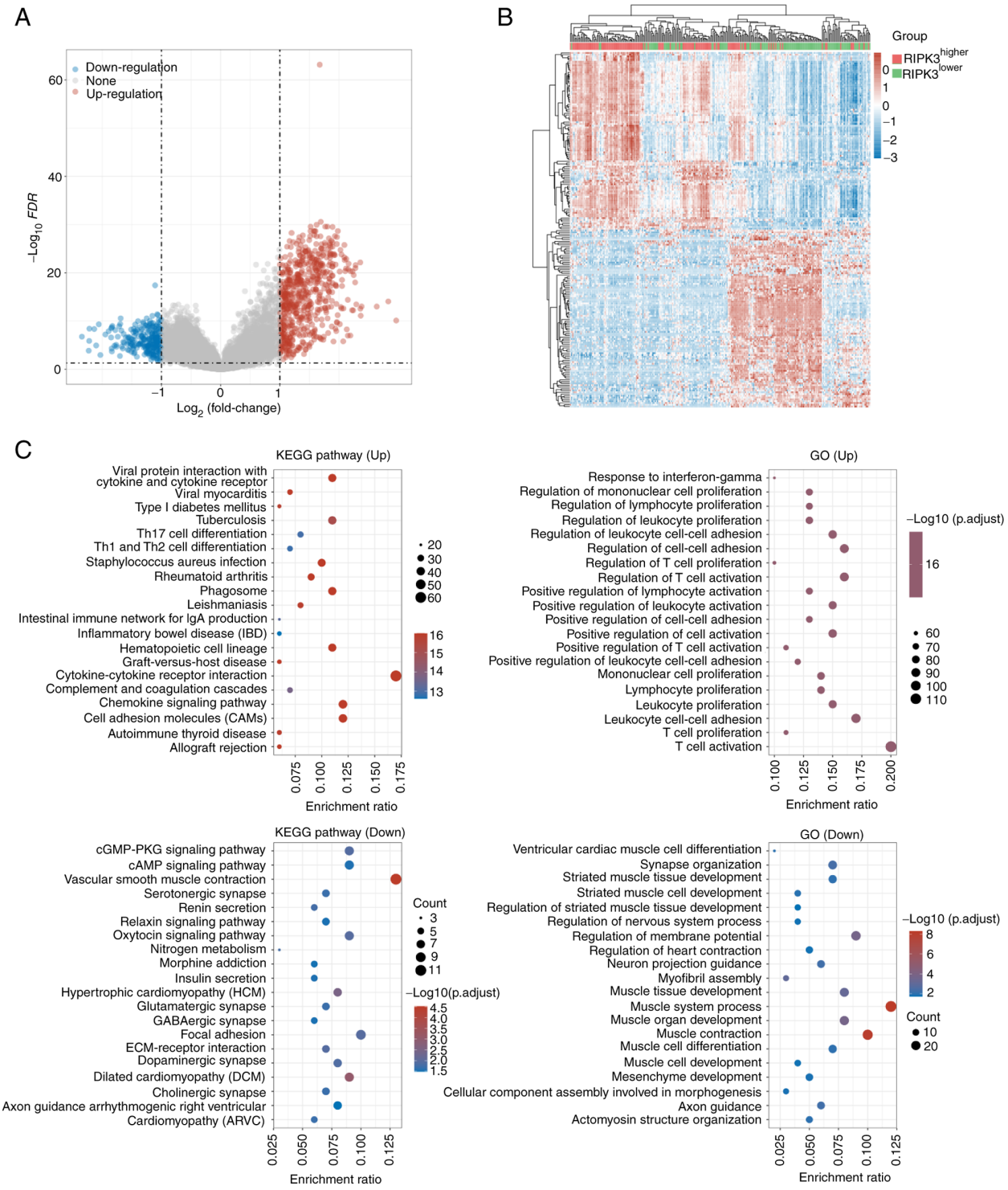

Figure 3. Expression profiles of the *RIPK3*^{higher} and *RIPK3*^{lower} groups from The Cancer Genome Atlas. (A) Volcano plot of transcriptome sequence data in the *RIPK3*^{higher} and *RIPK3*^{lower} groups. The red dots represent fold change >2 and FDR adjusted P<0.05, and the blue dots represent fold change <-2 and FDR adjusted P<0.05. (B) Unsupervised hierarchical clustering of 130 *RIPK3*^{higher} and 129 *RIPK3*^{lower} samples based on the top 50 up- and top 50 downregulated genes. Each column represents a sample, and differentially expressed genes are listed in rows. (C) KEGG and GO functional annotations of up- and down-regulated genes. *RIPK3*, receptor interacting serine/threonine kinase 3; KEGG, Kyoto Encyclopedia of Genes and Genomes; GO, Gene Ontology; FDR, false discovery rate.

suggesting its involvement in the regulation of immune checkpoints in these cell types.

Sarcoma is an aggressive malignant cancer with strong genetic and epigenetic components (24,25). Several publications have reported that mutations or genetic variations contribute to sarcoma; however, none of these variants are located within or near *RIPK3*. Furthermore, a search for mutations in TCGA datasets identified <10 *RIPK3* mutations in sarcoma cases, with no significant difference compared with the control group (data not shown). This finding indicates that *RIPK3* is not a trigger factor for sarcoma but is indirectly involved in disease regulation. This point was also supported by the epigenetic findings

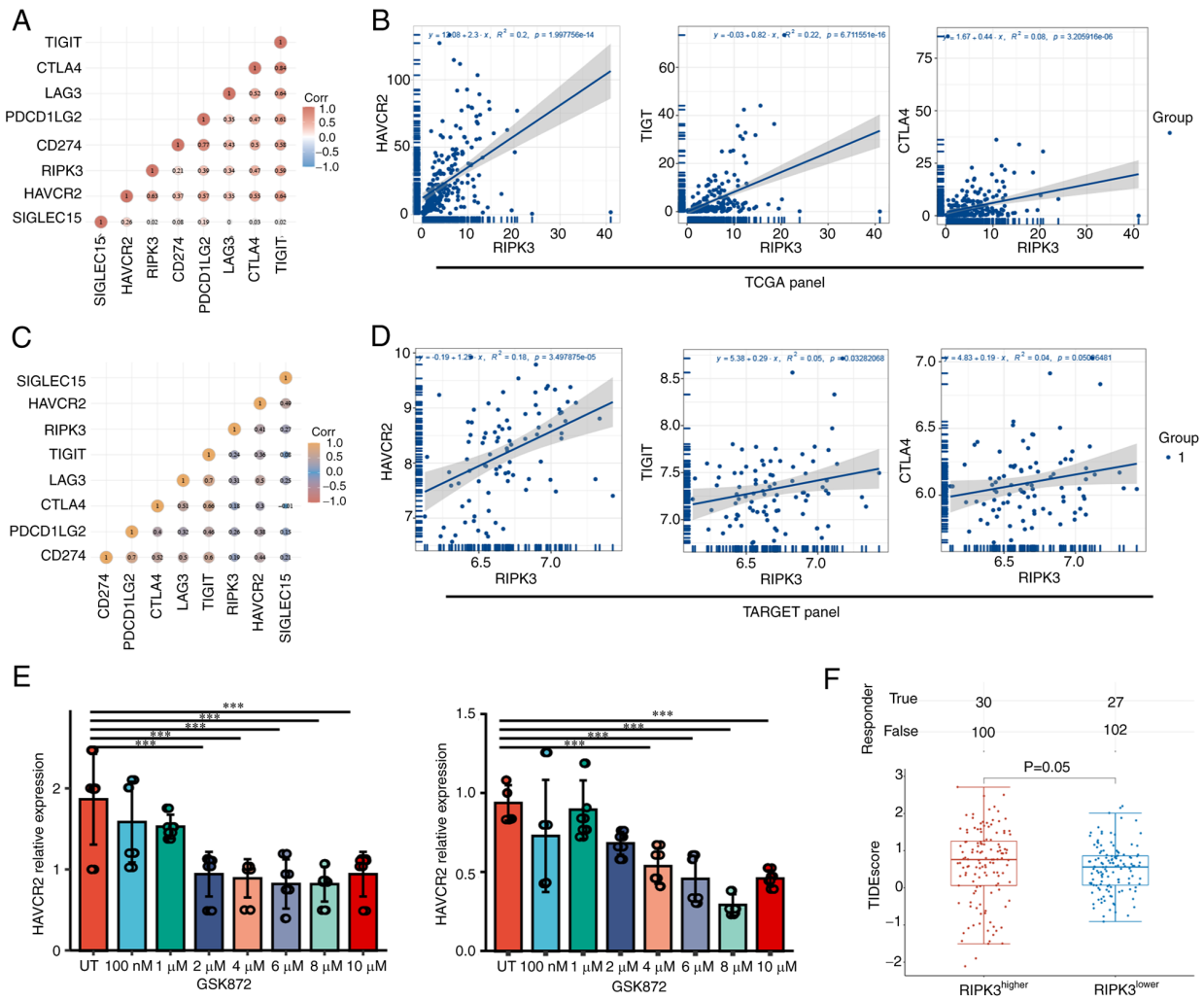

Figure 4. *RIPK3* may modulate the immune checkpoint through *HAVCR2*. (A) Correlation matrix and (B) Spearman's correlation analysis for *RIPK3* and immune checkpoint genes in The Cancer Genome Atlas. (C) Correlation matrix and (D) Spearman's correlation analysis for *RIPK3* and immune checkpoint genes in the Therapeutically Applicable Research To Generate Effective Treatments database. (E) *HAVCR2* expression in cells treated with the *RIPK3* inhibitor GSK872. Data were analyzed using one-way ANOVA followed by Dunnett's post hoc test. (F) Immune checkpoint blockade response, represented by TIDE scores, in the *RIPK3*^{higher} and *RIPK3*^{lower} groups. Data were analyzed using Wilcoxon's rank-sum test. ***P<0.001. *RIPK3*, receptor interacting serine/threonine kinase 3; *TIGIT*, T cell immunoreceptor with Ig and ITIM domains; *CTLA4*, cytotoxic T-lymphocyte associated protein 4; *LAG3*, lymphocyte-activation 3; *PDCD1LG2*, lymphocyte-activation 3 and programmed cell death 1 ligand 2; *HAVCR2*, hepatitis A virus cellular receptor 2; *SIGLEC15*, sialic acid binding Ig like lectin 15; TIDE, Tumor Immune Dysfunction and Exclusion; UT, untreated.

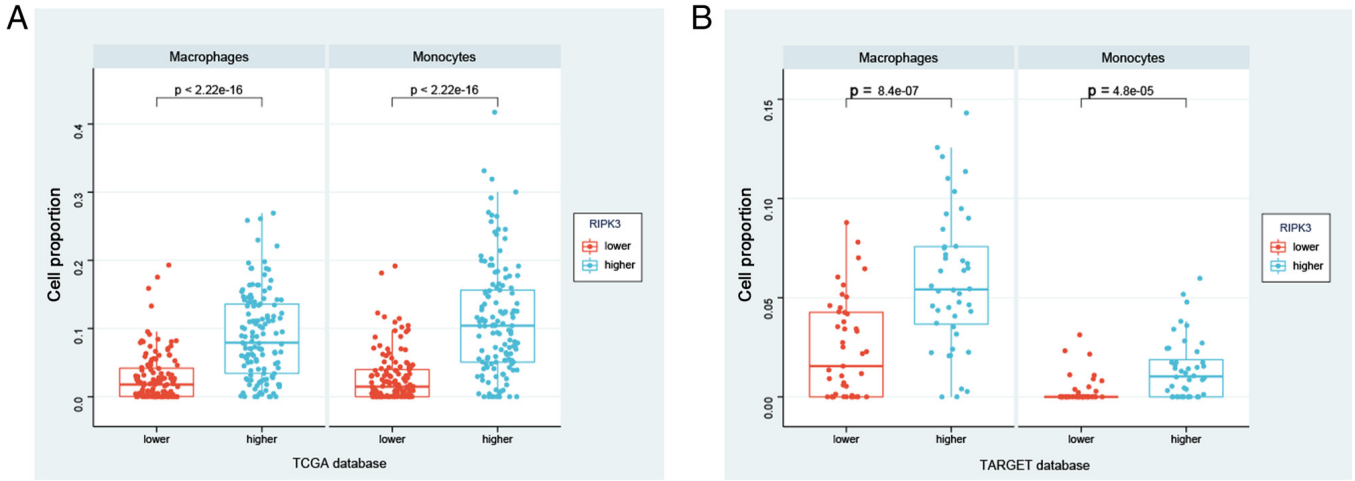

Figure 5. Immune cell infiltration in the *RIPK3*^{higher} and *RIPK3*^{lower} groups. Macrophages and monocytes show strong cell infiltration in the *RIPK3*^{higher} group in data from (A) TCGA and (B) TARGET. Two-sample t-tests were used to calculate the significance. *RIPK3*, receptor interacting serine/threonine kinase 3; TCGA, The Cancer Genome Atlas; TARGET, Therapeutically Applicable Research To Generate Effective Treatments.

of sarcoma. In a previous study, the DNA methylation level of *RIPK3* was found to be associated with a poor prognosis in osteosarcoma (26). In line with the aforementioned findings, the TCGA data analysis in the present study revealed improved survival and prognosis in the osteosarcoma groups with higher *RIPK3* expression. DNA methylation would be expected to suppress the expression of *RIPK3*, and the methylation of *RIPK3* could potentially serve as a therapeutic or survival predictor. Interestingly, another study observed that upregulation of *RIPK3* in U2OS osteosarcoma cells led to cell death when *RIPK3*-overexpressing U2OS cells were treated with 5-aminolevulic acid-mediated photodynamic therapy (27).

By comparing the gene expression profile of the $RIPK3^{higher}$ and $RIPK3^{lower}$ groups, 603 up- and 260 downregulated genes were identified. The number of genes with increased expression was 2.3-fold that of decreased genes, leading to the hypothesis that *RIPK3* could be universally involved in the modulation of gene expression, not just the expression of one or two target genes such as *HAVCR2*. Based on this hypothesis, it was considered that *RIPK3* may function as a transcription factor, although no supporting data are available to support this. Most importantly, the differentially expressed genes were involved in the pathways '*Staphylococcus aureus* infection' and 'cytokine-cytokine receptor interaction' (28). Furthermore, the top upregulated gene *TMC8* has been demonstrated to be a risk factor for head and neck squamous cancer (16) and renal cell carcinoma (29), while the top downregulated gene *TMEM97* is a transmembrane protein with largely unknown functions. The role of *TMEM97* in cancer appears to be diverse. It may be a putative tumor suppressor for pancreatic or prostate cancer (30), but it has also been shown to be associated with progression and poor survival in squamous cell carcinoma of the lung (18,31) and breast cancer (32). These genes and pathways have been confirmed as critical factors in sarcoma and other cancer types, indicating that *RIPK3* is a modulator of these biological processes.

An inflammatory microenvironment increases the risk of promoting tumors by mediating immune checkpoints in various types of cancer (33,34). Coupled with *RIPK1*, *RIPK3* induces cell death by assembling necrosomes, which is dependent on the presence of caspase-8 and occurs in a cell-type-specific manner (8). Apoptosis proteins (IAPs) are E3 ubiquitin ligases that ubiquitinate *RIPK1* or *RIPK2*, inducing an inflammatory response by the NF-κB or MAPK signalling pathways, suppressing the formation of the *RIPK3* necroptosis-inducing complex, or inhibiting the inflammatory pathways activated by the *RIPK1-RIPK3* complex (35). IAP antagonists, also known as Smac mimetics, have been shown to effectively sensitize cells from osteosarcomas and kill these cells following the administration of low levels of TNF-α. However, this function was not found to be dependent on the expression level of *RIPK3* in the cells, indicating that *RIPK3* might not act through classical inflammatory pathways (36). *RIPK3* has also shown inflammation-modulating effects in certain types of immune cells, such as monocytes and macrophages (37); however neither of these cell types were assayed in sarcomas conducted by Shekhar *et al* (36).

Another critical point is the immune checkpoint *HAVCR2*, which was first identified as an immune suppressor (38), is widely expressed in various cancer cells and can be induced by macrophage colony-stimulating factor. As the present study lacks functional data, it is not possible to evaluate whether *RIPK3* directly regulates the inflammatory response through *HAVCR2*. However, we hypothesize that this is likely due to the critical role of *RIPK3* in the activation of inflammation, the prediction of improved survival in cases with higher *HAVCR2* and the implied role of *HAVCR2* in tumor suppression as a target of cancer immunotherapy.

In conclusion, the present study analyzed TCGA data and identified that *RIPK3* was associated with improved survival of sarcoma, mostly likely through the immune checkpoint *HAVCR2*. The study findings suggest that *RIPK3*, as a critical molecular marker of necroptosis and apoptosis, serves as an immune regulator in sarcoma, which expands our understanding of disease etiology. This previously unreported finding will help us to better understand the etiology and treatment of sarcoma.

Acknowledgements

The authors would like to thank Professor Fusheng Zhou (Anhui Medical University, Hefei, China) for their statistical assistance.

Funding

This project was supported by the Affiliated Hospital of Yangzhou University.

Availability of data and materials

All data generated or analyzed during this study are included in this published article.

Authors' contributions

JD conceived the project and designed the study. CQ wrote the manuscript and performed most of the statistical analysis. DW helped to perform the statistical analysis, write the draft, and revise and approve the final version of the manuscript. All authors read and approved the final version of the manuscript. CQ and JD confirm the authenticity of all the raw data.

Ethics approval and consent to participate

Not applicable.

Patient consent for publication

Not applicable.

Competing interests

The authors declare that they have no competing interests.

References

1. Popovich JR, Kashyap S and Cassaro S: Sarcoma. In: StatPearls. Treasure Island (FL), 2022.
2. Bui NQ, Wang DS and Hiniker SM: Contemporary management of metastatic soft tissue sarcoma. Curr Probl Cancer 43: 289-299, 2019.
3. Howitt BE, Sholl LM, Dal Cin P, Jia Y, Yuan L, MacConaill L, Lindeman N, Kuo F, Garcia E, Nucci MR and Quade BJ: Targeted genomic analysis of mullerian adenosarcoma. J Pathol 235: 37-49, 2015.

4. Mirabello L, Zhu B, Koster R, Karlins E, Dean M, Yeager M, Gianferante M, Spector LG, Morton LM, Karyadi D, *et al*: Frequency of pathogenic germline variants in cancer-susceptibility genes in patients with osteosarcoma. JAMA Oncol 6: 724-734, 2020.
5. Koelsche C, Schrimpf D, Stichel D, Sill M, Sahm F, Reuss DE, Blattner M, Worst B, Heilig CE, Beck K, *et al*: Sarcoma classification by DNA methylation profiling. Nat Commun 12: 498, 2021.
6. Steele CD and Pillay N: The genomics of undifferentiated sarcoma of soft tissue: Progress, challenges and opportunities. Semin Cancer Biol 61: 42-55, 2020.
7. Cancer Genome Atlas Research Network. Electronic address: elizabeth.demicco@sinaihealthsystem.ca; Cancer Genome Atlas Research Network: Comprehensive and integrated genomic characterization of adult soft tissue sarcomas. Cell 171: 950-965. e28, 2017.
8. Jensen S, Seidelin JB, LaCasse EC and Nielsen OH: SMAC mimetics and RIPK inhibitors as therapeutics for chronic inflammatory diseases. Sci Signal 13: eaax8295, 2020.
9. Duan X, Liu X, Liu N, Huang Y, Jin Z, Zhang S, Ming Z and Chen H: Inhibition of keratinocyte necroptosis mediated by RIPK1/RIPK3/MLKL provides a protective effect against psoriatic inflammation. Cell Death Dis 11: 134, 2020.
10. Otsubo K, Maeyashiki C, Nibe Y, Tamura A, Aonuma E, Matsuda H, Kobayashi M, Onizawa M, Nemoto Y, Nagaishi T, *et al*: Receptor-Interacting Protein Kinase 3 (RIPK3) inhibits autophagic flux during necroptosis in intestinal epithelial cells. FEBS Lett 594: 1586-1595, 2020.
11. Wu S, Xu C, Xia K, Lin Y, Tian S, Ma H, Ji Y, Zhu F, He S and Zhang X: Ring closure strategy leads to potent RIPK3 inhibitors. Eur J Med Chem 217: 113327, 2021.
12. Karlsson J, Holmquist Mengelbier L, Ciornei CD, Naranjo A, O'Sullivan MJ and Gisselsson D: Clear cell sarcoma of the kidney demonstrates an embryonic signature indicative of a primitive nephrogenic origin. Genes Chromosomes Cancer 53: 381-391, 2014.
13. Ravi R, Noonan KA, Pham V, Bedi R, Zhavoronkov A, Ozerov IV, Makarev E, Artemov A, Wysocki PT, Mehra R, *et al*: Bifunctional immune checkpoint-targeted antibody-ligand traps that simultaneously disable TGFβ enhance the efficacy of cancer immunotherapy. Nat Commun 9: 741, 2018.
14. Zeng D, Li M, Zhou R, Zhang J, Sun H, Shi M, Bin J, Liao Y, Rao J and Liao W: Tumor microenvironment characterization in gastric cancer identifies prognostic and immunotherapeutically relevant gene signatures. Cancer Immunol Res 7: 737-750, 2019.
15. Wang J, Sun J, Liu LN, Flies DB, Nie X, Toki M, Zhang J, Song C, Zarr M, Zhou X, *et al*: Siglec-15 as an immune suppressor and potential target for normalization cancer immunotherapy. Nat Med 25: 656-666, 2019.
16. Tirosh I, Izar B, Prakadan SM, Wadsworth MH II, Treacy D, Trombetta JJ, Rotem A, Rodman C, Lian C, Murphy G, *et al*: Dissecting the multicellular ecosystem of metastatic melanoma by single-cell RNA-seq. Science 352: 189-196, 2016.
17. Lin B, Wang S, Yao Y, Shen Y and Yang H: Comprehensive co-expression analysis reveals TMC8 as a prognostic immune-associated gene in head and neck squamous cancer. Oncol Lett 22: 498, 2021.
18. Ding H, Gui XH, Lin XB, Chen RH, Cai HR, Fen Y and Sheng YL: Prognostic value of MAC30 expression in human pure squamous cell carcinomas of the lung. Asian Pac J Cancer Prev 17: 2705-2710, 2016.
19. Mandal P, Berger SB, Pillay S, Moriwaki K, Huang C, Guo H, Lich JD, Finger J, Kasparcova V, Votta B, *et al*: RIP3 induces apoptosis independent of pronecrotic kinase activity. Mol Cell 56: 481-495, 2014.
20. André S, Picard M, Cezar R, Roux-Dalvai F, Alleaume-Butaux A, Soundaramourty C, Cruz AS, Mendes-Frias A, Gotti C, Leclercq M, *et al*: T cell apoptosis characterizes severe Covid-19 disease. Cell Death Differ 29: 1486-1499, 2022.
21. Chen X, Zhu R, Zhong J, Ying Y, Wang W, Cao Y, Cai H, Li X, Shuai J and Han J: Mosaic composition of RIP1-RIP3 signalling hub and its role in regulating cell death. Nat Cell Biol 24: 471-482, 2022.
22. Jiang P, Gu S, Pan D, Fu J, Sahu A, Hu X, Li Z, Traugh N, Bu X, Li B, *et al*: Signatures of T cell dysfunction and exclusion predict cancer immunotherapy response. Nat Med 24: 1550-1558, 2018.
23. Racle J, de Jonge K, Baumgaertner P, Speiser DE and Gfeller D: Simultaneous enumeration of cancer and immune cell types from bulk tumor gene expression data. Elife 6: e26476, 2017.
24. Bieging KT, Mello SS and Attardi LD: Unravelling mechanisms of p53-mediated tumour suppression. Nat Rev Cancer 14: 359-370, 2014.
25. Liu Y, Sánchez-Tilló E, Lu X, Clem B, Telang S, Jenson AB, Cuatrecasas M, Chesney J, Postigo A and Dean DC: Rb1 family mutation is sufficient for sarcoma initiation. Nat Commun 4: 2650, 2013.
26. Tian W, Li Y, Zhang J, Li J and Gao J: Combined analysis of DNA methylation and gene expression profiles of osteosarcoma identified several prognosis signatures. Gene 650: 7-14, 2018.
27. Coupienne I, Fettweis G and Piette J: RIP3 expression induces a death profile change in U2OS osteosarcoma cells after 5-ALA-PDT. Lasers Surg Med 43: 557-564, 2011.
28. Tuohy JL, Somarelli JA, Borst LB, Eward WC, Lascelles BD and Fogle JE: Immune dysregulation and osteosarcoma: Staphylococcus aureus downregulates TGF-β and heightens the inflammatory signature in human and canine macrophages suppressed by osteosarcoma. Vet Comp Oncol 18: 64-75, 2020.
29. Castro FA, Ivansson EL, Schmitt M, Juko-Pecirep I, Kjellberg L, Hildesheim A, Gyllensten UB and Pawlita M: Contribution of TMC6 and TMC8 (EVER1 and EVER2) variants to cervical cancer susceptibility. Int J Cancer 130: 349-355, 2012.
30. Ramalho-Carvalho J, Gonçalves CS, Graça I, Bidarra D, Pereira-Silva E, Salta S, Godinho MI, Gomez A, Esteller M, Costa BM, *et al*: A multiplatform approach identifies miR-152-3p as a common epigenetically regulated onco-suppressor in prostate cancer targeting TMEM97. Clin Epigenetics 10: 40, 2018.
31. Ding H, Gui X, Lin X, Chen R, Ma T, Sheng Y, Cai H and Fen Y: The prognostic effect of MAC30 expression on patients with non-small cell lung cancer receiving adjuvant chemotherapy. Technol Cancer Res Treat 16: 645-653, 2017.
32. Xiao M, Li H, Yang S, Huang Y, Jia S, Wang H, Wang J and Li Z: Expression of MAC30 protein is related to survival and clinicopathological variables in breast cancer. J Surg Oncol 107: 456-462, 2013.
33. Workenhe ST, Nguyen A, Bakhshinyan D, Wei J, Hare DN, MacNeill KL, Wan Y, Oberst A, Bramson JL, Nasir JA, *et al*: De novo necroptosis creates an inflammatory environment mediating tumor susceptibility to immune checkpoint inhibitors. Commun Biol 3: 645, 2020.
34. Bagchi S, Yuan R and Engleman EG: Immune checkpoint inhibitors for the treatment of cancer: Clinical impact and mechanisms of response and resistance. Annu Rev Pathol 16: 223-249, 2021.
35. Gyrd-Hansen M and Meier P: IAPs: From caspase inhibitors to modulators of NF-kappaB, inflammation and cancer. Nat Rev Cancer 10: 561-574, 2010.
36. Shekhar TM, Miles MA, Gupte A, Taylor S, Tascone B, Walkley CR and Hawkins CJ: IAP antagonists sensitize murine osteosarcoma cells to killing by TNFα. Oncotarget 7: 33866-33886, 2016.
37. Wu L, Chung JY, Cao T, Jin G, Edmiston WJ III, Hickman S, Levy ES, Whalen JA, Abrams ES, Degterev A, *et al*: Genetic inhibition of RIPK3 ameliorates functional outcome in controlled cortical impact independent of necroptosis. Cell Death Dis 12: 1064, 2021.
38. Kandel S, Adhikary P, Li G and Cheng K: The TIM3/Gal9 signaling pathway: An emerging target for cancer immunotherapy. Cancer Lett 510: 67-78, 2021.